parGeMSLR: A Parallel Multilevel Schur Complement Low-Rank Preconditioning and Solution Package for General Sparse Matrices

Tianshi Xu[a,*], Vassilis Kalantzis[b], Ruipeng Li[c], Yuanzhe Xi[d], Geoffrey Dillon[e], Yousef Saad[a]

[a]Department of Computer Science and Engineering, University of Minnesota, Minneapolis, MN 55455
[b]Thomas J. Watson Research Center, IBM Research, Yorktown Heights, NY 10598
[c]Center for Applied Scientific Computing, Lawrence Livermore National Laboratory, P.O. Box 808, L-561, Livermore, CA 94551
[d]Department of Mathematics, Emory University, Atlanta, GA 30322
[e]Department of Mathematics, University of South Carolina, Columbia, SC 29208

arXiv:2205.03224v1 [cs.MS] 4 May 2022

Abstract

This paper discusses parGeMSLR, a C++/MPI software library for the solution of sparse systems of linear algebraic equations via preconditioned Krylov subspace methods in distributed-memory computing environments. The preconditioner implemented in parGeMSLR is based on algebraic domain decomposition and partitions the symmetrized adjacency graph recursively into several non-overlapping partitions via a p-way vertex separator, where p is an integer multiple of the total number of MPI processes. From a numerical perspective, parGeMSLR builds a Schur complement approximate inverse preconditioner as the sum between the matrix inverse of the interface coupling matrix and a low-rank correction term. To reduce the cost associated with the computation of the approximate inverse matrices, parGeMSLR exploits a multilevel partitioning of the algebraic domain. The parGeMSLR library is implemented on top of the Message Passing Interface and can solve both real and complex linear systems. Furthermore, parGeMSLR can take advantage of hybrid computing environments with in-node access to one or more Graphics Processing Units. Finally, the parallel efficiency (weak and strong scaling) of parGeMSLR is demonstrated on a few model problems arising from discretizations of 3D Partial Differential Equations.

Keywords: Schur complement, low-rank correction, distributed-memory preconditioner, sparse non-Hermitian linear systems, Graphics Processing Units

1. Introduction

This paper discusses a distributed-memory library for the iterative solution of systems of linear algebraic equations of the form

$$Ax = b, \tag{1}$$

where the matrix $A \in \mathbb{C}^{n\times n}$ is large, sparse, and (non-)Hermitian. Problems of this form typically originate from the discretization of a Partial Differential Equation in 2D or 3D domains.

Iterative methods solve (1) by a preconditioned Krylov subspace iterative methods [1, 2], e.g., preconditioned Conjugate Gradient [1], if A is Hermitian and positive-definite, or GMRES [3] if A is non-Hermitian. The role of the preconditioner is to cluster the eigenvalues in an effort to accelerate the convergence of Krylov subspace method. For example, an efficient right preconditioner M transforms (1) into the preconditioned system $AM^{-1}(Mx) = b$, where M^{-1} can be applied inexpensively. An additional requirement is that the setup and application of the operator M^{-1} should be easily parallelizable.

Similarly to Krylov subspace methods, algebraic multigrid (AMG) methods are another widely-used class of iterative solvers [4]. AMG uses the ideas of interpolation and restriction to build multilevel preconditioners that eliminate the smooth error components. AMG is provably optimal for Poisson-like problems on regular meshes where the number of iterations to achieve convergence almost stays constant as the problem size increases. This property leads to appealing weak scaling results of AMG in distributed-memory computing environments [5, 6, 7]. However, AMG can fail when applied either to indefinite problems or irregular meshes. It is worth mentioning that AMG can also be used as a preconditioner in the context of Krylov subspace methods.

For general sparse linear systems, a well-known class of general-purpose preconditioners is that of Incomplete LU (ILU) factorization preconditioners [8, 9, 1]. Here, the matrix A is approximately factored as $A \approx LU$ where L is lower triangular and U is upper triangular, and the preconditioner is defined as $M = LU$. Applying M^{-1} then consists of two triangular substitutions. ILU preconditioners can be applied to a greater selection of problems than AMG, including indefinite problems such as discretized Helmholtz equations [10, 11], and their robustness can be improved by modified/shifted ILU strategies [12, 13, 14]. On the other hand, the scalability of ILU preconditioned Krylov subspace methods is typically inferior com-

*The work of the first and the last author was supported by the National Science Foundation (NSF) grant DMS-1912048. The work of the fourth author was supported by the NSF grant OAC-2003720. This work was performed under the auspices of the U.S. Department of Energy by Lawrence Livermore National Laboratory under Contract DE-AC52-07NA27344 (LLNL-JRNL-830724)

pared to AMG. In particular, even for Poisson-like problems, the number of iterations to achieve convergence by ILU preconditioned Krylov subspace methods increases with respect to the matrix size. Moreover, the sequential nature of triangular substitutions limit the parallel efficiency of ILU preconditioners implemented on distributed-memory systems, and recent efforts have been focusing on improving their scalability, e.g., see [15, 16, 17].

The parallel efficiency of ILU preconditioners can be enhanced by domain decomposition (DD), where the original problem is decomposed into several subdomains which correspond to different blocks of rows of the coefficient matrix A. The simplest DD-based ILU approach is the block-Jacobi ILU preconditioner, where a local ILU is performed on each local submatrix. Since this method ignores all of the off-diagonal matrices corresponding to inter-domain couplings, its convergence rate tends to become slower as the number of subdomains increases, and several strategies have been proposed to handle the inter-domain couplings in order to improve the convergence rate. Restricted Additive Schwarz (RAS) methods expand the local matrix by a certain level to gain a faster convergence rate at the cost of losing some memory scalability [18]. Global factorization ILU methods factorize local rows corresponding to interior unknowns first, after which a global factorization of the couplings matrix is applied based on some graph algorithms [19, 20]. These methods use partial ILU techniques with dropping [21, 22], incomplete triangular solve [23], and low-rank approximation [24] to form the Schur complement system and can be generalized into multilevel ILU approaches [21, 22, 24]. When the Finite Element method is used and the elements are known, two-level DD methods including BDDC [25] and FETI-DP [26, 27], as well as the GenEO preconditioner [28] are also have been shown to be effective approaches. We note that an additional strategy is to combine approximate direct factorization techniques with low-rank representation of matrix blocks [29], PasTix [30], and DDLR [31]. When the matrix A is SPD, it is possible to reduce the size of the Schur complement matrix without introducing any fill-in, e.g., see SpaND [32].

Other preconditioning strategies that can be implemented on distributed-memory environments include the (factorized) sparse approximate inverse preconditioners [33, 34, 35, 36, 37], polynomial preconditioners [38], and rank-structured preconditioners [39, 40, 41, 42]; see also [43] for a distributed-memory hierarchical solver. Some of the these techniques can be further compounded with AMG, as "smoothers", or ILU-based preconditioners. For example, a combination of SLR [44] and polynomial preconditioning is discussed in [38].

1.1. Contributions of this paper

This paper discusses the implementation of a distributed-memory library, termed[1] `parGeMSLR`, for the iterative solution of sparse systems of linear algebraic equations in large-scale distributed-memory computing environments. `parGeMSLR`[2] is written in C++, and communication among different processor groups is achieved by means of the Message Passing Interface standard (MPI). The `parGeMSLR` library is based on the Generalized Multilevel Schur complement Low-Rank (GeMSLR) algorithm described in [24]. GeMSLR applies a multilevel partitioning of the algebraic domain, and the variables associated with each level are divided into either interior or interface variables. The multilevel structure is built by applying a p-way graph partitioner to partition the induced subgraph associated with the interface variables of the preceding level. Once the multilevel partitioning is completed, GeMSLR creates a separate Schur complement approximate inverse at each level. Each approximate inverse is the sum of two terms, with the first term being an approximate inverse of the interface coupling matrix, and the second term being a low-rank correction which aims at bridging the gap between the first term and the actual Schur complement matrix inverse associated with that level. Below, we summarize the main features of the `parGeMSLR` library:

1. **Scalability**. `parGeMSLR` extends the capabilities of low-rank-based preconditioners, such as GeMSLR, by recursively partitioning the algebraic domain into levels which have the same number of partitions. In turn, this leads to enhanced scalability when running on distributed-memory environments.
2. **Robustness and complex arithmetic**. In contrast to ILU preconditioners, the numerical method implemented in `parGeMSLR` is less sensitive to indefiniteness and can be updated on-the-fly without discarding previous computational efforts. Additionally, `parGeMSLR` supports complex arithmetic and thus can be utilized to solve complex linear systems such as those originating from the discretization of Helmholtz equations.
3. **Hybrid hardware acceleration**. GPU acceleration is supported in several iterative solver libraries aiming to speed-up the application of preconditioners such as AMG or ILU, e.g., `hypre` [45], `PARALUTION` [46], `ViennaCL` [47], `HIFLOW` [48], `PETSc` [49], and `Trilinos` [50]. A number of direct solver libraries including `STRUMPACK` [51, 52, 53] and SuperLU_DIST [54] also provide GPU support. Similarly, `parGeMSLR` can exploit one or more GPUs by offloading any computation for which the user provides a CUDA interface.

This paper is organized as follows. Section 2 discusses low-rank correction preconditioners and provides an algorithmic description of `parGeMSLR`. Section 3 provides details on the multilevel reordering used by `parGeMSLR`. Section 4 presents in-depth discussion and details related to the implementation and parallel performance aspects of `parGeMSLR`. Section 5 demonstrates the performance of `parGeMSLR` on distributed-memory environments. Finally, our concluding remarks are presented in Section 6.

[1] The abbreviation of the library is derived by the complete name "parallel Generalized multilevel Schur complement Low-Rank preconditioner"

[2] The source code can be found in https://github.com/Hitenze/pargemslr

2. Schur complement approximate inverse preconditioners via low-rank corrections

This section discussed the main idea behind (multilevel) Schur complement preconditioners enhanced by low-rank corrections, e.g., see [55, 44, 24, 56].

2.1. The Schur complement viewpoint

Let the linear system $Ax = b$ be permuted as

$$A_0 x = P^T A P (P^T x) = P^T b, \tag{2}$$

where P is an $n \times n$ permutation matrix such that

$$A_0 = \begin{bmatrix} B & F \\ E & C \end{bmatrix} = \begin{bmatrix} B^{(1)} & & & & F^{(1)} \\ & B^{(2)} & & & F^{(2)} \\ & & \ddots & & \vdots \\ & & & B^{(p)} & F^{(p)} \\ E^{(1)} & E^{(2)} & \cdots & E^{(p)} & C \end{bmatrix},$$

and the matrices $B^{(i)}$, $F^{(i)}$, and $E^{(i)}$ are of size $d_i \times d_i$, $d_i \times s$, and $s \times d_i$, respectively. The matrix C is of size $s \times s$, and the matrix partitioning satisfies $d + s = \sum_{j=1}^{j=p} d_j + s_j = n$. Such matrix permutations can be computed by partitioning the adjacency graph of the matrix $|A| + \left|A^T\right|$ into $p \in \mathbb{N}$ non-overlapping partitions and reordering the unknowns/equations such that the variables associated with the d interior nodes across all partitions are ordered before the variables associated with the s interface nodes.

Following the above notation, the linear system in (2) can be written in a block form

$$\begin{bmatrix} B & F \\ E & C \end{bmatrix} \begin{bmatrix} u \\ v \end{bmatrix} = \begin{bmatrix} f \\ g \end{bmatrix}, \tag{3}$$

where $u, f \in \mathbb{R}^d$ and $v, g \in \mathbb{R}^s$. Once the solution in (3) is computed, the solution x of the original, non-permuted system of linear algebraic equations $Ax = b$ can be obtained by the inverse permutation $x = P \begin{bmatrix} u \\ v \end{bmatrix}$. Throughout the rest of this section we focus on the solution of the system in (3).

Following a block-LDU factorization of the matrix A_0, the permuted linear system in (2) can be written as

$$\begin{bmatrix} I & \\ EB^{-1} & I \end{bmatrix} \begin{bmatrix} B & \\ & S \end{bmatrix} \begin{bmatrix} I & B^{-1}F \\ & I \end{bmatrix} \begin{bmatrix} u \\ v \end{bmatrix} = \begin{bmatrix} f \\ g \end{bmatrix}, \tag{4}$$

where $S = C - EB^{-1}F$ denotes the *Schur complement matrix*. The solution of (3) is then equal to

$$\begin{bmatrix} u \\ v \end{bmatrix} = \begin{bmatrix} I & -B^{-1}F \\ & I \end{bmatrix} \begin{bmatrix} B^{-1} & \\ & S^{-1} \end{bmatrix} \begin{bmatrix} I & \\ -EB^{-1} & I \end{bmatrix} \begin{bmatrix} f \\ g \end{bmatrix},$$

which requires: *a*) the solution of two linear systems with the block-diagonal matrix B, and *b*) the solution of one linear system with the the Schur complement matrix S. Note that since the matrix B is block-diagonal, the associated linear systems are decoupled into p independent systems of linear algebraic equations. Assuming a distributed-memory computing environment with p separate processor groups, each system of linear algebraic equations can be solved in parallel by means of applying a direct solver locally in each separate process.

In several real-world applications, e.g., those involving the discretization of PDEs on three-dimensional domains, solving the systems of linear algebraic equations with matrices B and S through a direct solver is generally impractical, primarily due to the large computational and memory cost associated with forming and factorizing the Schur complement matrix. An alternative then is to solve the linear systems with matrices B and S inexactly. For example, the solution of linear systems with matrix B can be computed approximately by replacing its exact LU factorization with an incomplete threshold LU (ILUT) [8]. Likewise, the exact Schur complement can be sparsified by discarding entries below a certain threshold value or located outside a pre-determined pattern [22, 57] The approximate factorizations of the matrices B and S can be combined to form an approximate LDU factorization of (4) which can be then used as a preconditioner in a Krylov subspace iterative solver such as GMRES.

2.2. Schur complements and low-rank corrections

One of the main drawbacks associated with incomplete factorizations is that they can not be easily updated if one needs a more accurate preconditioner unless the iterative ParILUT [15, 16] works for the problem and is used. Moreover, their robustness can be limited when the matrix A is indefinite. For such scenarios, it has been advocated to add a *low-rank correction term* to enhance the efficiency of the Schur complement preconditioner, without discarding the previously computed incomplete factorizations. The low-rank enhancement implemented in `parGeMSLR` follows the GeMSLR multilevel preconditioner [24], a non-Hermitian extension of [44, 56]. Other approaches based on low-rank corrections can be found in [55, 58].

The GeMSLR preconditioner expresses the Schur complement matrix as

$$S = (I - EB^{-1}FC^{-1})C = (I - G)C, \tag{5}$$

where $G = EB^{-1}FC^{-1}$. Consider now the complex Schur decomposition $G = WRW^H$, where the $s \times s$ matrix W is unitary and the $s \times s$ matrix R is upper-triangular such that its diagonal entries contain the eigenvalues of matrix G. Plugging the latter in (5) results to

$$S = (I - WRW^H)C = W(I - R)W^H C,$$

from which we can write the inverse of the Schur complement matrix as (Sherman-Morrison-Woodbury formula):

$$S^{-1} = C^{-1} + C^{-1}W[(I - R)^{-1} - I]W^H. \tag{6}$$

Following (6), a system of linear equations with the Schur complement matrix requires the solution of a system of linear equations with matrix C, as well as matrix-vector multiplications and triangular matrix inversions with matrices W/W^H and $(I - R)^{-1}$, respectively. The product of matrices $W[(I - R)^{-1} - I]W^H$

is a Schur decomposition by itself, with corresponding eigenvalues $\gamma_i/(1-\gamma_i)$, $i = 1, \ldots, s$, where γ_i denotes the i-th eigenvalue of the matrix G. Therefore, as long as the eigenvalues of the latter matrix are not located close to one, the matrix $C(S^{-1} - C^{-1}) = W[(I-R)^{-1} - I]W^H$ can be approximated by a low-rank matrix, i.e., S^{-1} is approximately equal to C^{-1} plus some low-rank correction.

The expression in (6) can be transformed into a practical preconditioner if the matrix $W[(I-R)^{-1} - I]W^H$ is replaced by a rank-k approximation, where $k \in \mathbb{N}$ is generally a user-given parameter. More specifically, let W_k denote the $s \times k$ matrix which holds the leading k Schur vectors of matrix G, and let R_k denote the $k \times k$ leading principal submatrix of matrix R. Then, the GeMSLR approximate inverse preconditioner is equal to

$$M^{-1} = C^{-1} + C^{-1} W_k [(I - R_k)^{-1} - I] W_k^H \approx S^{-1}. \tag{7}$$

2.3. Computations with an incomplete factorization of B

For large-scale problems, computing an exact factorization of the block-diagonal matrix B can be quite expensive. Instead, what is typically available is an ILUT factorization $LU \approx B$. Therefore, instead of computing a rank-k Schur decomposition of matrix G, in practice we approximate a truncated Schur decomposition of the matrix $\widehat{G} = E(U^{-1}L^{-1})FC^{-1}$. Let then

$$\widehat{G}\widehat{V}_m = \widehat{V}_m \widehat{H}_m + \beta_m \widehat{v}_{m+1} e_m^H,$$

denote an m-length Arnoldi relation obtained with matrix $\widehat{G}$, where $[\widehat{V}_m, \widehat{v}_{m+1}]^H [\widehat{V}_m, \widehat{v}_{m+1}] = I$, and $\widehat{H}_m$ is upper-Hessenberg. Moreover, let $\widehat{H}_m = QTQ^H$ denote the complex Schur decomposition of matrix $\widehat{H}_m$. The low-rank correction term used in GeMSLR is of the form $\widehat{W}_k[(I - \widehat{R}_k)^{-1} - I]\widehat{W}_k^H$, where $T_k \in \mathbb{R}^{k \times k}$ denotes the $k \times k$ leading principal submatrix of matrix T, and $\widehat{W}_k = \widehat{V}_m Q_k$, where $Q_k \in \mathbb{R}^{s \times k}$ denotes the matrix holding the k leading Schur vectors of matrix $\widehat{H}_m$.

2.4. Multilevel extensions

For large-scale, high-dimensional problems, the application of the matrix C^{-1} by means of an LU factorization of matrix C can still be expensive; especially when the value of p is too large, leading to large vertex separators. The idea suggested in [56, 31], and employed by GeMSLR, is to take advantage of the purely algebraic formulation developed in the previous section and apply C^{-1} inexactly by using the Schur complement low-rank preconditioner described in the previous section. In fact, this approach can be repeated more than once, leading to a multilevel preconditioner.

More specifically, let $l_{ev} \in \mathbb{N}$ denote the number of levels, and define the sequence of matrices

$$A_l = P_{l-1} C_{l-1} P_{l-1} = \begin{bmatrix} B_l & F_l \\ E_l & C_l \end{bmatrix}, \quad C_{-1} = A, \quad l = 0, 1, \ldots, l_{ev} - 1, \tag{8}$$

where the matrix B_l is block-diagonal with p on-diagonal matrix blocks. The 2×2 block matrix partition of each matrix A_l is obtained by partitioning the adjacency graph of the matrix $|C_{l-1}| + |C_{l-1}^T|$ into p non-overlapping partitions and reordering the unknowns/equations such that the variables associated with the interior nodes across all partitions are ordered before the variables associated with the interface nodes of the adjacency graph. The matrix C_{l-1} is then permuted in-place through the $s_{l-1} \times s_{l-1}$ permutation matrix P_{l-1}, where s_{l-1} denotes the size of the matrix C_{l-1}.

The solution of a system of linear algebraic equations with matrix A_l as the coefficient matrix and $\begin{bmatrix} f_l^T & g_l^T \end{bmatrix}^T$ as the right-hand side, can be computed as

$$\begin{bmatrix} u_l \\ v_l \end{bmatrix} = \begin{bmatrix} I & -B_l^{-1} F_l \\ & I \end{bmatrix} \begin{bmatrix} B_l^{-1} & \\ & S_l^{-1} \end{bmatrix} \begin{bmatrix} I & \\ -E_l B_l^{-1} & I \end{bmatrix} \begin{bmatrix} f_l \\ g_l \end{bmatrix},$$

where $S_l = C_l - E_l B_l^{-1} F_l$ denotes the $s_l \times s_l$ Schur complement matrix associated with the l-th level, where $s_l \in \mathbb{N}$ denotes the size of the matrix C_l. Instead of computing the exact LU factorizations of matrices B_l and S_l, the preconditioner implemented in the `parGeMSLR` library substitutes $B_l^{-1} \approx (L_l U_l)^{-1}$, where $L_l U_l$ denotes an ILUT factorization of matrix B_l, and

$$S_l^{-1} \approx C_l^{-1} + C_l^{-1} W_{l,k} [(I - R_{l,k})^{-1} - I] W_{l,k}^H, \tag{9}$$

where $\widehat{W}_{l,k}$ denotes the matrix which holds the approximate leading k Schur vectors of the matrix $\widehat{G}_l = E_l^T U_l^{-1} L_l^{-1} F_l C_l^{-1}$, and $\widehat{R}_{l,k}$ denotes the approximation of the $k \times k$ leading principal submatrix of the matrix $\widehat{R}_l$ that satisfis the Schur decomposition $\widehat{G}_l = \widehat{W}_l \widehat{R}_l \widehat{W}_l^H$. Algorithm 1 summarizes the above discussion ("setup phase") in the form of an algorithm. Notice that the recursion stops at level $l_{ev} - 1$, and an ILUT of the matrix $C_{l_{ev}-1}$ is computed explicitly.

Algorithm 1 Parallel GeMSLR Setup

1: **procedure** pGeMSLRSetup(A, l_{ev})
2: Generate l_{ev}-level structure by Algorithm 3.
3: **for** l from 0 to $l_{ev} - 1$ **do**
4: Compute ILU factorization $L_l U_l \approx B_l$.
5: Compute matrices $\widehat{W}_{l,k}$ and $\widehat{R}_{l,k}$.
6: If $l = l_{ev} - 1$, compute an ILUT factorization $L_{l_{ev}-1} U_{l_{ev}-1} \approx C_{l_{ev}-1}$; exit.
7: **end for**
8: **end procedure**

Algorithm 2 outlines the procedure associated with the application of the GeMSLR preconditioner ("solve phase"). At each level, the preconditioning step consists of a forward and backward substitution with the ILUT triangular factors of B_l, followed by the application of the rank-k correction term. When $l = l_{ev} - 1$, there is no low-rank correction term applied, since this is the last level. Moreover, when $l = 0$ (root level), it is possible to enhance the GeMSLR preconditioner by applying a few steps of right preconditioned GMRES. Note though that these iterations are performed with the inexact Schur complement $\widehat{S}_l = C_l - E_l (U^{-1} L^{-1}) F_l$.

3. Multilevel reordering

This section outlines the multilevel reordering approach implemented in the `parGeMSLR` library. For simplicity, we focus

Algorithm 2 Standard Parallel GeMSLR Solve

procedure pGeMSLRSolve(b, l)
  Apply reordering $\begin{bmatrix} b_1 \\ b_2 \end{bmatrix} = P_{l-1} b$.
  Solve $z_1 = U_l^{-1} L_l^{-1} b_1$.
  Compute $z_2 = b_2 - E_l z_1$.
  if $l = 0$ **then**
    Solve $\widehat{S}_l y_2 = z_2$ by right preconditioned GMRES.
  else
    Compute $u_2 = \widehat{W}_{l,k}[(I - \widehat{R}_{l,k})^{-1} - I]\widehat{W}_{l,k}^H z_2$
    Call y_2 = pGeMSLRSolve($u_2 + z_2, l + 1$).
  end if
  Compute $y_1 = z_1 - U_l^{-1} L_l^{-1} F_l y_2$.
  Apply reordering $q = P_{l-1} \begin{bmatrix} y_1 \\ y_2 \end{bmatrix}$.
  return x
end procedure

on symmetric reorderings obtained by applying a p-way vertex separator to the adjacency graph associated with the matrices $|C_{l-1}| + |C_{l-1}^T|$, $l = 0, \ldots, l_{ev} - 1$, $C_{-1} = A$, [59, 60, 61, 62]. In particular, given a graph $G = (V, E)$, a p-way vertex separator computes a separator $\mathcal{S} \subset V$ and p non-overlapping (disjoint) sets $V_1, \ldots, V_p \subset V$ such that $V_1 \cup \ldots \cup V_p \cup \mathcal{S} = V$ and there are no edges connecting the sets V_i and V_j when $i \neq j$.

Algorithm 3 Parallel GeMSLR Reordering

procedure pGeMSLRReordering(A, l_{ev})
  Set $C_{-1} \equiv A$.
  for l from 0 to $l_{ev} - 1$ **do**
    Apply p-way partitioning to the graph associated with the matrix $|C_{l-1}| + |C_{l-1}^T|$.
    Set $A_l = P_{l-1} C_{l-1} P_{l-1} = \begin{bmatrix} B_l & F_l \\ E_l & C_l \end{bmatrix}$.
  end for
  return
end procedure

3.1. Hierarchical Interface Decomposition

The GeMSLR preconditioner relies on a Hierarchical Interface Decomposition (HID) [63] to reduce the setup cost of the ILU and low-rank correction parts associated with the setup phase of the preconditioner. The main idea behind HID is to partition the adjacency graph of $|A| + |A^T|$ into $2^{l_{ev}}$ partitions via nested dissection with a recursion depth of l_{ev}. The vertex separators at level l are disjoint with each other since they are divided by vertex separators from higher levels. When ordered by levels, the global permutation of matrix A will have a block-diagonal structure with $2^{l_{ev}-l}$ blocks at level $0 \leq l \leq l_{ev} - 1$, i.e., the number of diagonal blocks at each level reduce by a factor of two.

3.2. Multilevel partitioning through p-way vertex separators

In contrast to low-rank correction preconditioners such as MSLR and GeMSLR [56, 24], the main goal of `parGeMSLR` is to sustain good parallel efficiency, and thus HID is not appropriate.[3] Instead, the default approach in `parGeMSLR` is to partition the adjacency graph by a multi-level partitioner where each level consists of p partitions and a vertex separator. The latter choice results to a *fixed number of p partitions at each level*, and thus load balancing is generally much better than that obtained using HID.

A high-level description can be found in Algorithm 3. At the root level ($l = 0$), the graph associated with the matrix $|A| + |A^T|$, is partitioned into p subdomains with a p-way vertex separator, resulting to p non-overlapping connected components and their associated vertex separator. The multilevel partitioner then proceeds to the next level, $l = 1$, and applies the p-way vertex partitioner to the induced subgraph associated with the vertex separator at level $l = 0$. This leads to a second set of p non-overlapping connected components and a new, albeit smaller vertex separator. The p-way vertex partitioner is then applied again to the induced subgraph associated with the vertex separator obtained at level $l = 1$, etc. The procedure continues until either level $l_{ev} - 1$ is reached, or the vertex separator at the current level l has so few vertices that it can not be further partitioned into p non-overlapping partitions.

An illustration of a three-level, four-way partitioner applied to a three-dimensional algebraic domain (a unit cube) is shown in Figure 1. The leftmost subfigure shows the $p = 4$ separate partitions obtained by the application of the four-way vertex partitioner as well as the vertex separator itself (shown in white color) at level $l = 0$. This vertex separator, which consists of four two-dimensional faces, forms the algebraic object to be partitioned at level $l = 1$, and the partitioning is shown in the middle subfigure, where this time the vertex separator is a one-dimensional object. Finally, at level $l = 2$, the most recent vertex separator is further partitioned into four independent partitions, leading to a new vertex separator which consists of only three vertices; see the rightmost subfigure.

In addition to the above illustration, Figure 2 plots the sparsity pattern of a Finite Difference discretization of the Laplace operator on a three-dimensional domain, after reordering its rows and columns according to a p-way, multilevel reordering with $l_{ev} = 4$ and $p = 4$ (left). A zoom-in of the submatrix associated with the permutation of the vertex separators is also shown (right). Note that in this particular example, the last level has already too few variables to be partitioned any further. In addition to the global, multilevel permutation, each matrix B_l can be further permuted locally by a reordering scheme such as reverse Cuthill-Mckee (RCM) algorithm or approximate minimal degree algorithm (AMD) [64, 65] to reduce the fill-ins.

4. Implementation details of `parGeMSLR`

The `parGeMSLR` library consists of three main modules: *a*) a distributed-memory reordering scheme, *b*) a Krylov subspace

[3] Nonetheless, HID is offered in `parGeMSLR`.

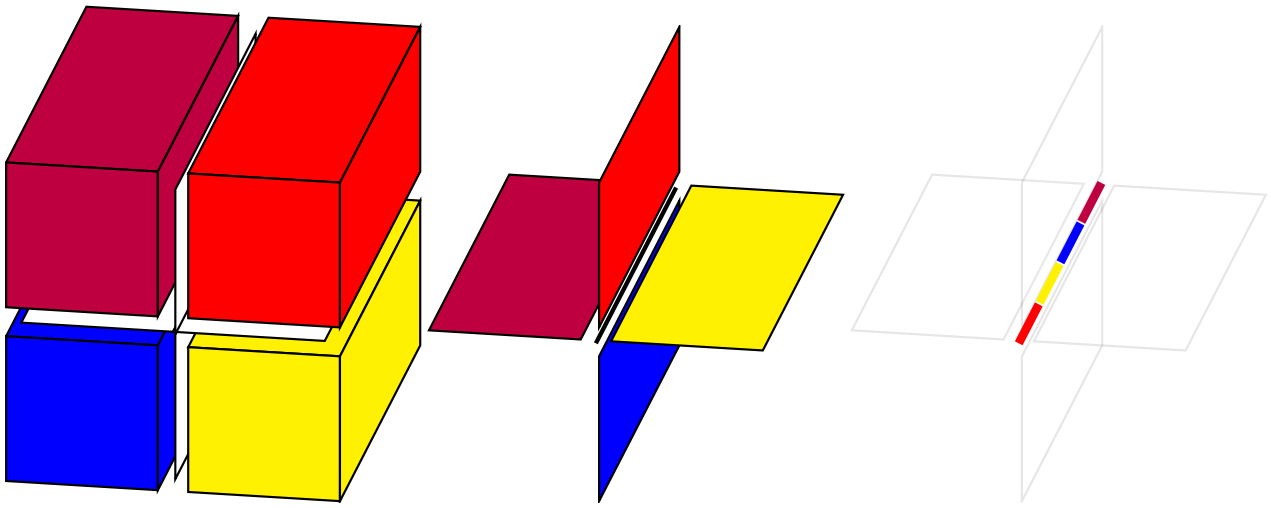


Figure 1: Left: a three-dimensional domain partitioned into $p = 4$ subdomains. The vertex separator consists of four faces, with each face located between neighboring subdomains. Center: partitioning of the root-level separator into $p = 4$ subdomains. Right: partitioning of the vertex separator at the second level.

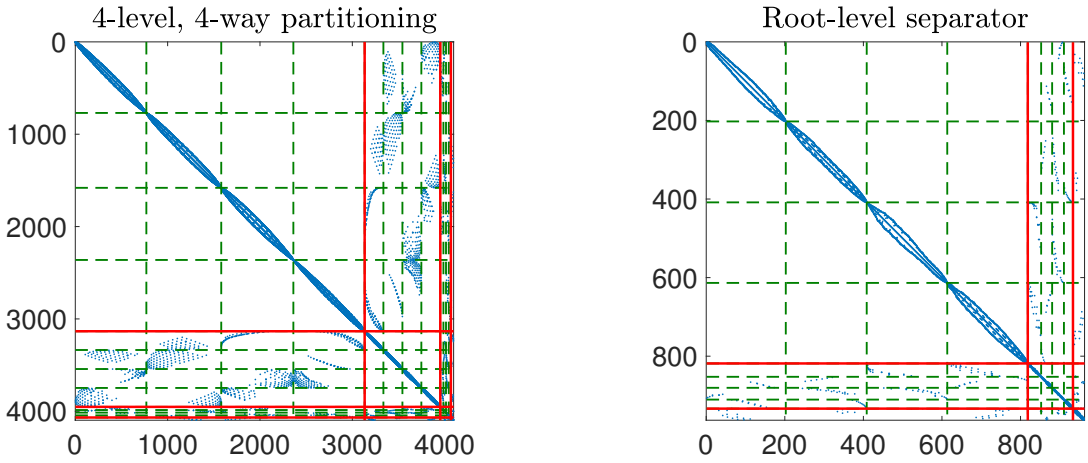


Figure 2: Left: global permutation of matrix A following a multilevel partitioning with $l_{ev} = 4$ and $p = 4$. Right: zoom-in at the submatrix associated with the permutation of the vertex separators (right-bottom submatrix of the left subfigure).

iterative accelerator, and c) the setup and application of the GeMSLR preconditioner. The first module was described in greater detail in Section 3, and is implemented through a distributed-memory partitioner such as ParMETIS. Additional point-to-point communication between neighboring partitions, as well as a single All-to-All message are required (to find the new neighbors of each partition post-partitioning). Next, we focus on the implementation of the other two modules in a distributed-memory environment where different processor groups communicate via MPI.

4.1. Distributed-memory operations in Krylov accelerators

Standard, non-preconditioned Krylov iterative methods are built on top of simple linear algebraic operations such as matrix-vector multiplication, vector scaling and additions, and DOT products. Iterative solvers such as GMRES or FGMRES also require the solution of small-scale ordinary linear-least squares problems which are typically solved redundantly in each MPI process.

Assuming that the data associated with the system of linear algebraic equations we wish to solve is already distributed across the different MPI process via 1D row distribution, AXPY operations can be executed locally and involve no communication overhead. On the other hand, sparse matrix-vector multiplications and DOT products involve either point-to-point or collective communication. In particular, assume $n_p \in \mathbb{N}$ MPI processes. A DOT product then requires a collective operation, i.e., `MPI_Allreduce`, to sum the n_p local DOT products. The cost of this operation is roughly $O(log(n_p)\alpha)$, where $\alpha \in \mathbb{R}$ denotes the maximum latency between two MPI process. On the other hand, a matrix-vector multiplication with the coefficient matrix of the linear system requires point-to-point communication, where the local matrix-vector product in each MPI process consists of operations using local data, as well as data associated with MPI processes which are assigned to neighboring subdomains, e.g., see [66] for additional details and recent advances.

4.2. Preconditioner setup and application

The main module of `parGeMSLR` is the setup of the GeMSLR preconditioner, followed by the application of the latter at each iteration of the Krylov subspace iterative solver of choice. Following a multilevel partition into l_{ev} levels (see Section 3), the setup phase of the GeMSLR preconditioner associated with each level $l = 0, 1, \ldots, l_{ev} - 1$, is further divided into two separate submodules: *a*) computation of an ILUT factorization $B_l \approx L_l U_l$, and *b*) computation of an approximate rank-k Schur decomposition of the matrix $\widehat{G}_l = E_l^T U_l^{-1} L_l^{-1} F_l C_l^{-1}$.

Let us consider each one of the above two tasks separately. Recall that the data matrix at each level $0 \leq l \leq l_{ev} - 1$ has the following pattern

$$A_l = P_l C_{l-1} P_l = \begin{bmatrix} B_l & F_l \\ E_l & C_l \end{bmatrix} = \begin{bmatrix} B_l^{(1)} & & & & F_l^{(1)} \\ & B_l^{(2)} & & & F_l^{(2)} \\ & & \ddots & & \vdots \\ & & & B_l^{(p)} & F_l^{(p)} \\ E_l^{(1)} & E_l^{(2)} & \cdots & E_l^{(p)} & C_l \end{bmatrix}.$$

Now, without loss of generality, assume that each partition is assigned to a separate MPI process. Figure 3 (left) plots a graphical illustration of the data layout of matrix A_l obtained by a permutation using $p = 4$, across four different MPI processes. Data associated with separate MPI processes are presented with a different color. Notice that the right-bottom submatrix denotes the matrix C_l representing the coupling between variables of the vertex separator at level l. Computing an ILUT factorization of the matrix B_l decouples into p independent ILUT subproblems $B_l^{(j)} \approx L_l^{(j)} U_l^{(j)}$, $j = 1, \ldots, p$, and thus no communication overhead is enabled. On the other hand, the computation of the low-rank correction term requires the application of several steps of the Arnoldi iteration, and requires communication overhead.

More specifically, the Arnoldi iteration requires communication among the various MPI processes to compute matrix-vector multiplications with the iteration matrix $\widehat{G}_l$, as well as to maintain orthogonality of the Krylov basis. When the latter is achieved by means of standard Gram-Schmidt, Arnoldi requires one `MPI_Allreduce` operation at each iteration. Similarly, the matrix-vector multiplication between $\widehat{G}_l$ and a vector z is equal to

$$\begin{bmatrix} E_l^{(1)} & \cdots & E_l^{(p)} \end{bmatrix} \begin{bmatrix} L_l^{(1)} U_l^{(1)} & & \\ & \ddots & \\ & & L_l^{(p)} U_l^{(p)} \end{bmatrix}^{-1} \begin{bmatrix} F_l^{(1)} \\ \vdots \\ F_l^{(p)} \end{bmatrix} C_l^{-1} z.$$

The computation of the product $C_l^{-1} z$ requires access to the incomplete ILUT factorizations and rank-k correction terms associated with all levels $l < \widehat{l} \leq l_{ev} - 1$. Therefore, the rank-$k$ correction terms are built in a bottom-up fashion, from $l = l_{ev} - 1$ to $l = 0$, so that level l has immediate access to the data associated with all levels $\widehat{l} > l$. Once the matrix-vector multiplication $C_l^{-1} z$ is computed, the matrix-vector multiplication with matrix F_l is computed with trivial parallelism among the MPI processes, and the same holds for the linear system solutions with matrices $L_l^{(j)}$, $U_l^{(j)}$, $j = 1, \ldots, p$. Finally, the matrix-vector multiplication with matrix E_l requires an `MPI_Allreduce` operation. Note though that if we were to replace vertex separators with edge separators (this option is included in `parGeMSLR`) then the latter multiplication would also be communication-free.

Finally, applying the preconditioner requires embarrassingly parallel triangular substitutions with the ILUT factorizations of the block-diagonal matrices B_l as well as dense matrix-vector multiplications with matrices $\widehat{W}_{l,k}$, $\widehat{W}_{l,k}^H$, and $(I - \widehat{R}_{l,k})^{-1}$. A matrix-vector multiplication with the matrix $\widehat{W}_{l,k}$ requires no communication among the MPI processes, while a matrix-vector multiplication with the matrix $\widehat{W}_{l,k}^H$ requires an `MPI_Allreduce` operation at level l. Finally, the matrix-vector multiplication with the $k \times k$ matrix $(I - \widehat{R}_{l,k})^{-1}$ is performed redundantly in each MPI process since k is typically pretty small.

4.2.1. Communication overhead analysis

In this section we focus on the communication overhead associated with setting up and applying the preconditioner implemented in `parGeMSLR`. For simplicity, we assume that the number of MPI processes n_p is equal to the number of partitions p at each level. The main parameters of the preconditioner are the number of levels l_{ev} and the value of rank k.

Let us first consider the application of m Arnoldi iterations to compute the matrices $\widehat{W}_{l,k}$ and $(I - \widehat{R}_{l,k})^{-1}$ for some $0 \leq l \leq l_{ev} - 1$. As was discussed in the previous section, computing matrix-vector products with the matrix $\widehat{G}_l$ requires communication only during the application of the matrices E_l and C_l^{-1}. In turn, the latter requires computations with the distributed matrices C_{l+1}^{-1}, $W_{l+1,k}^H$, C_{l+2}^{-1}, $W_{l+2,k}^H$, and so on, until we reach level $l_{ev} - 1$ where an ILUT of the matrix $C_{l_{ev}-1}$ is computed explicitly. Thus, a matrix-vector multiplication with the matrix $\widehat{G}_l$ requires $l_{ev} - (l+1)$ (low-rank correction term) and $l_{ev} - l$ (C_l^{-1} recursion) `MPI_Allreduce` operations. In summary, an m-length Arnoldi cycle with standard Gram-Schmidt orthonormalization requires $(2l_{ev} - 2l + 1)m$ `MPI_Allreduce` operations, where we also accounted for the two `MPI_Allreduce` operations stemming by Gram-Schmidt and vector normalization at each iteration. This communication overhead is inversely proportional to the level index l. Accounting for all $l_{ev} - 1$ levels, the total communication overhead associated with the setup phase of the preconditioner amounts is bounded by $\delta(k) \sum_{l=0}^{l=l_{ev}-1} (2l_{ev} - 2l + 1)m$ `MPI_Allreduce` operations, where $\delta(k) \in \mathbb{N}$ denotes the maximum number of cycles performed by Arnoldi at any level. In `parGeMSLR`, the default cycle length is $m = 2k$ iterations. Finally, after the set up phase, one full application of the preconditioner implemented in the `parGeMSLR` library requires $2(l_{ev} - l) + 1$ `MPI_Allreduce` operations.

The analysis presented in this section demonstrates that the communication overhead associated with the construction of the GeMSLR preconditioner is directly proportional to an increase in the value of l_{ev}. On the other hand, increasing the value of l_{ev} can reduce the computational complexity associated with setting up the GeMSLR preconditioner in lower levels. Nonetheless, the value of l_{ev} can not be too large, especially when the value of p is large, since the size of the vertex separator reduces dramatically between successive levels (as is demonstrated in Figure 1).

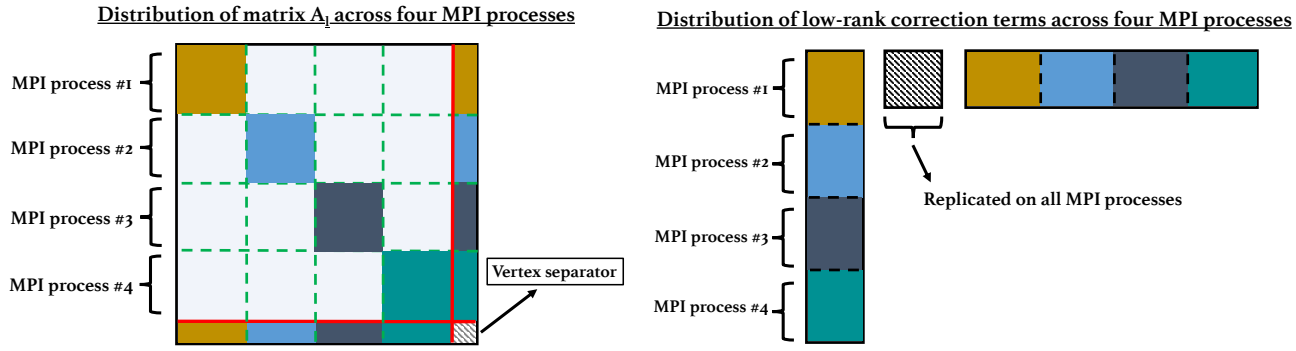


Figure 3: Left: layout of the matrix correction term across four MPI processes (same for any level $0 \leq l \leq l_{ev} - 1$). Right: layout of a rank-k correction term across four MPI processes (same for any level $0 \leq l < l_{ev} - 1$).

4.3. Applying $C_{l_{ev}-1}^{-1}$

Due to partitioning with a multilevel vertex separator, the matrix $C_{l_{ev}-1}$ forms a separate partition which is replicated among all MPI processes. Therefore, the simplest approach to apply $C_{l_{ev}-1}^{-1}$ is to do so approximately, through computing an ILUT redundantly in each MPI process. However, for large problems, this approach can quickly become impractical, even if a shared-memory variant of ILUT is considered [15]. On the other hand, applying a distributed-memory approach that requires communication among the MPI processes can lead to high communication overhead since the application of $C_{l_{ev}-1}^{-1}$ is the most common operation during the setup phase of the preconditioner.

`parGeMSLR` includes several[4] options to apply an approximation of $C_{l_{ev}-1}^{-1}$. The default option considered throughout our experiments is to apply $C_{l_{ev}-1}^{-1}$ approximately through a block-Jacobi approach where $C_{l_{ev}-1}$ is first permuted by reverse RCM and then replaced by its on-diagonal block submatrices while the rest of the entries are discarded. Generally speaking, dropping these entries of $C_{l_{ev}-1}^{-1}$ has minor effects since $C_{l_{ev}-1}$ is already close to being block-diagonal for modest values of l_{ev} (e.g., three or four) as was already demonstrated in Figure 1. By default, the number of retained on-diagonal blocks of matrix $C_{l_{ev}-1}$ is set equal to p. The approximate application of $C_{l_{ev}-1}^{-1}$ is then trivially parallel among the MPI processes, and each one of the retained on-diagonal blocks is applied through ILUT.

5. Numerical Experiments

In this section we demonstrate the parallel performance of `parGeMSLR`. We run our experiments on the Quartz cluster of Lawrence Livermore National Laboratory. Each node of Quartz has 128 GB memory and consists of 2 Intel Xeon E5-2695 CPUs with 36 cores in total. We use MVAPICH2 2.2.3, to compile `parGeMSLR` is compiled with MVAPICH2 2.2.3, following rank-to-core binding. By default, all of the experiments presented below are executed in double-precision.[5] On top of distributed-memory parallelism, `parGeMSLR` can take advantage of shared memory parallelism using either OpenMP or CUDA. The current version of `parGeMSLR` uses LAPACK for sequential matrix decompositions and ParMETIS for distributed graph partitioning [59]. A detailed documentation of `parGeMSLR` can be found in the "DOCS" directory of `https://github.com/Hitenze/pargemslr`. This documentation provides detailed information on how to compile and run `parGeMSLR`, and includes a detailed description of all command-line parameters as well as visualization of the source code hierarchy. Several test drivers, and a sample input file, are also included.

Throughout the rest of this section, we choose Flexible GMRES (FGMRES) with a fixed restart size of fifty as the outer iterative solver. The motivation for using FGMRES instead of GMRES is that the application of the preconditioner is subject to variations due to the application of the inner solver in step 9 of Algorithm 2. The stopping tolerance for the relative residual norm in FGMRES is set equal to $1.0\mathtt{e}-6$. Unless mentioned otherwise, the solution of the linear system $Ax = b$ will be equal to the vector of all ones with an initial approximation equal to zero. The low-rank correction term at each level consists of approximate Schur vectors such that the corresponding approximate eigenvalues are accurate to two digits of accuracy, and the restart cycle of thick-restart Arnoldi is equal to $2k$.

Our distributed-memory experiments focus on the parallel efficiency of `parGeMSLR` both when the problem size remains fixed and n_p increases (strong scaling) and the problem size increases at the same rate with n_p. In the case of weak scaling, the parallel efficiency is equal to $\frac{T_1}{T_{n_p}}$, where T_1 and T_{n_p} denote the wall-clock time achieved by the sequential and distributed-memory version (using n_p MPI processes) of `parGeMSLR`, respectively. Likewise, in the case of strong scaling, the parallel efficiency is equal to $\frac{T_1}{n_p T_{n_p}}$. In addition, we also compare `parGeMSLR` against: *a*) the BoomerAMG parallel implementation of the algebraic multigrid method in `hypre`, and *b*) the two-level SchurILU approach in [22]. The latter preconditioner uses partial ILU to form an approximation of the Schur com-

[4] See section 2.1 in `https://github.com/Hitenze/pargemslr/blob/main/ParGeMSLR/DOCS/Documentation.pdf`

[5] We note though that `parGeMSLR` supports both real and complex arithmetic, as well as both single and double precision.

plement matrix. The preconditioning step is then performed by applying GMRES with block-Jacobi preconditioning to solve the linear system associated with the sparsified Schur complement. The block-Jacobi preconditioner is applied through one step of ILUT, and our implementation of SchurILU is based on the parallel ILU(T) in hypre.

Throughout the rest of this section, we adopt the following notation:

- $\mathbf{n_p} \in \mathbb{N}$: total number of MPI processes.
- **fill** $\in \mathbb{R}$: ratio between the number of non-zero entries of the preconditioner and that of matrix A.
- **p-t** $\in \mathbb{R}$: preconditioner setup time. This includes the time required to compute the ILUT factorizations and low-rank correction terms in `parGeMSLR`.
- **i-t** $\in \mathbb{R}$: iteration time of FGMRES.
- **its** $\in \mathbb{N}$: total number of FGMRES iterations.
- **k** $\in \mathbb{N}$: number of low-rank correction terms at each level.
- **F**: flag signaling that FGMRES failed to converge within 1000 iterations.

5.1. A Model Problem

This section considers a Finite Difference discretization of the model problem

$$\begin{aligned} -\Delta u - cu &= f \text{ in } \Omega, \\ u &= 0 \text{ on } \partial\Omega. \end{aligned} \tag{10}$$

We consider a 7-pt stencil and set $\Omega = (0,1)^3$.

5.1.1. Weak scaling

Our first set of experiments studies the weak scaling efficiency of `parGeMSLR`. Since varying the values of l_{ev} and k lead to different convergence rates, we first consider the case where the number of FGMRES iterations is set equal to thirty, regardless of whether convergence was achieved or not. The problem size on each MPI process is fixed to 50^3, while the number of subdomains at each level is set equal to $8 \times n_p$. Moreover, the number of levels is varied as $l_{ev} \in \{2, 3\}$ while the rank of the low-rank correction terms is varied as $k \in \{0, 100, 200\}$.

Figure 4 plots the weak scaling efficiency of `parGeMSLR` on up to $n_p = 1,024$ MPI processes. The achieved efficiency is similar for both options of l_{ev} with a slightly higher efficiency observed for the case $l_{ev} = 3$. As expected, the highest efficiency achieved during the preconditioner setup phase was for the case $k = 0$, since there is no communication overhead stemming from the low-rank correction terms. Nonetheless, even in this case there is some loss in efficiency due to load imbalancing introduced by the ILUT factorizations at different levels. Regardless of the value of k, the efficiency of `parGeMSLR` drops the most when the number of MPI processes is small, regardless of the value of l_{ev}. This reduction is owed to the relatively large increase on the size of the local Schur complement versus when a larger number of MPI processes is utilized. Note though, although not reported in our experiments, that the weak scaling efficiency is typically much higher when each MPI process

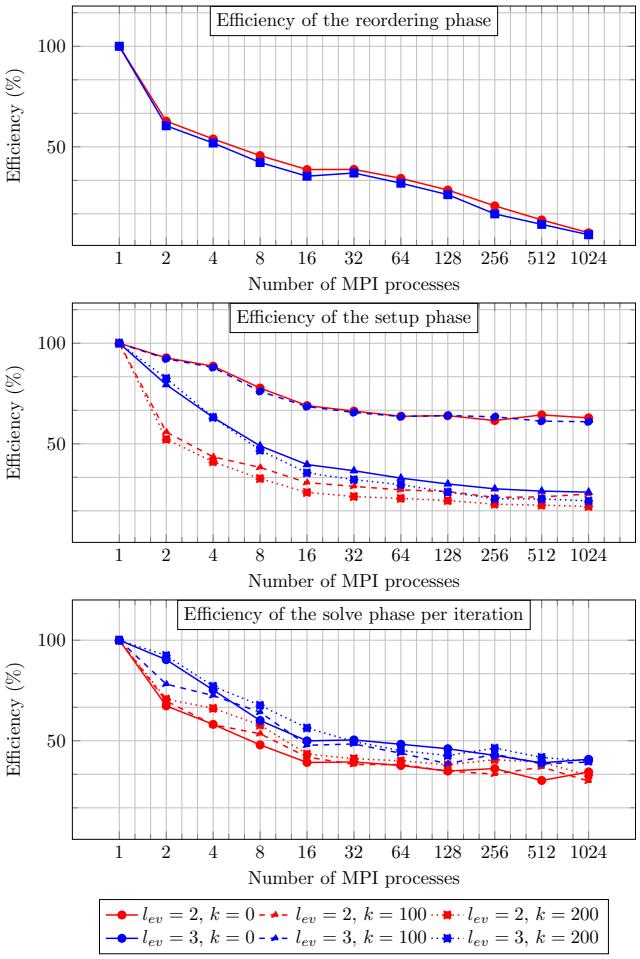


Figure 4: Weak scaling of `parGeMSLR` for the Poisson problem when the number of iterations performed by FGMRES is fixed to thirty, and the number of levels is set to $l_{ev} = 2$ and $l_{ev} = 3$. The number of unknowns on each MPI process is $125,000$, for a maximum problem size $n = 800 \times 400 \times 400$.

handles exactly one subdomain. Finally, the efficiency of the reordering phase is rather limited, since the wall-clock time requires to partition the graph associated with the matrix $|A|+|A^T|$ and permute the distributed matrix A increases as the problem size grows.

Figure 5 plots the weak scalability of `parGeMSLR` and two-level SchurILU, where this time we allow enough iterations in FGMRES until convergence. As previously, we use eight subdomains per MPI process, but this time we fix $l_{ev} = 3$ and $k = 10$. In summary, `parGeMSLR` is both faster and more scalable than SchurILU during the solve phase. Moreover, `parGeMSLR` also converges much faster than SchurILU, and the number of total FGMRES iterations increases only marginally with the problem size. On the other hand, the weak scaling of the preconditioner setup phase of `parGeMSLR` is impacted negatively as the problem size increases due to the need to perform more Arnoldi iterations to compute the low-rank correction terms.

5.1.2. Strong scaling

We now present strong scaling results obtained by solving (10) with `parGeMSLR` on a regular mesh of fixed size as the

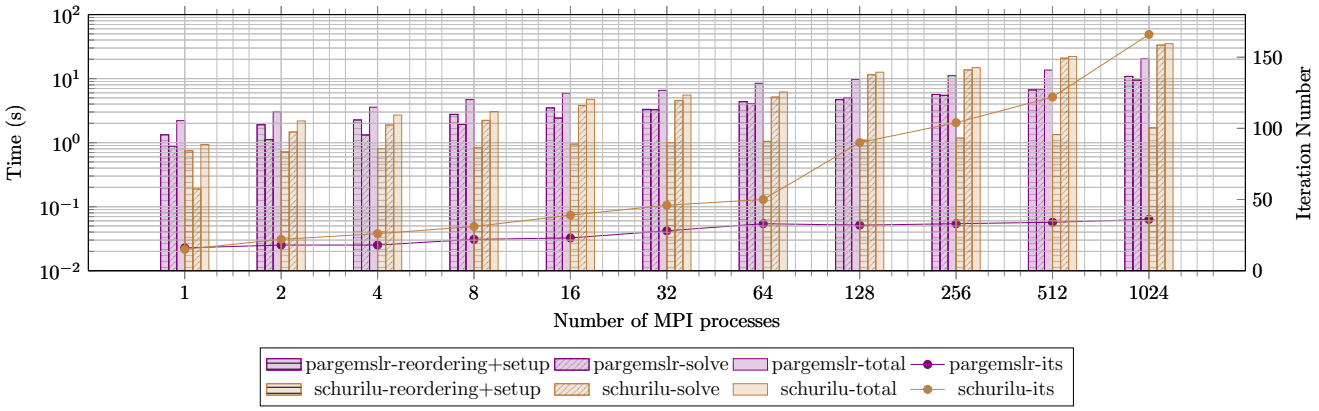


Figure 5: Weak scaling of `parGeMSLR` and SchurILU on Poisson problems. The number of unknowns on each MPI process is 125,000, for a maximum problem size $n = 800 \times 400 \times 400$.

numbers of MPI processes varies. More specifically, the size of the problem is fixed to $n = 320^3$ while the number of MPI processes varies up to $n_p = 1,024$. The values of l_{ev} and k are varied as previously.

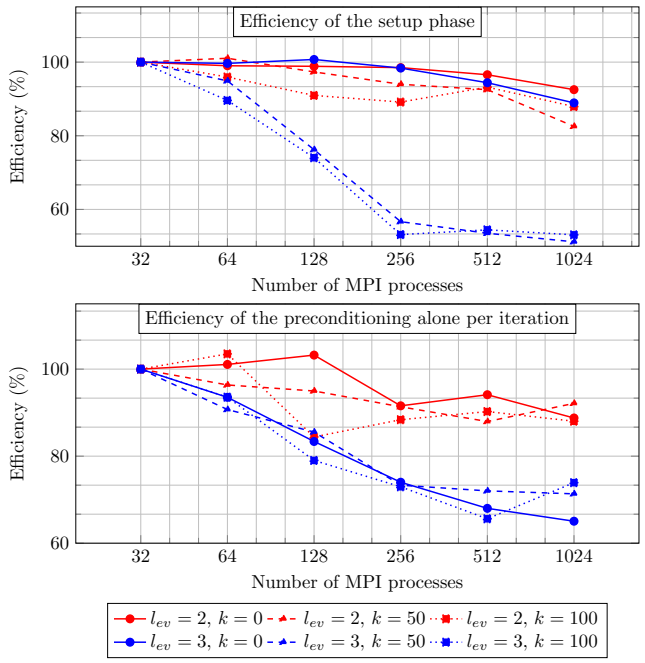


Figure 6: Strong scaling results for Poisson problems of size $n = 320^3$. The number of subdomains is set equal to 2048 in all levels.

Figure 6 plots the strong scaling of `parGeMSLR`. In contrast to the weak scaling case, setting $l_{ev} = 2$ leads to higher efficiency during both the setup and application phases of the preconditioner. The reason for this behavior is twofold. First, increasing the value of l_{ev} generally deteriorates the effectiveness of the preconditioner unless k is large and the threshold used in the local ILUT factorizations is small. Second, decreasing the value of l_{ev} enhances strong scalability since it leads to smaller communication overheads (i.e., recall the discussion in Section 4). As a general remark, we note that the setup phase of `parGeMSLR` generally becomes more expensive in terms of floating-point arithmetic operations as l_{ev} decreases, thus although scalability deteriorates as l_{ev} increases, the actual wall-clock time might actually decrease if the number of MPI processes used is small.

5.2. General Problems

This section discusses the performance of `parGeMSLR` on a variety of problems in engineering.

5.2.1. Unstructured Poisson problem on a crooked pipe

We consider the numerical solution of (10) where $f = 1$ and $c = 0$ on a 3D crooked pipe mesh. The problem is discretized by second-order Finite Elements using the MFEM library [67, 68] with local uniform and parallel mesh refinement. The initial approximation of the solution is set equal to zero. We visualize the (inhomogeneous) mesh using the package GLVis [69] in Figure 7. Our experiments consider different refinement levels

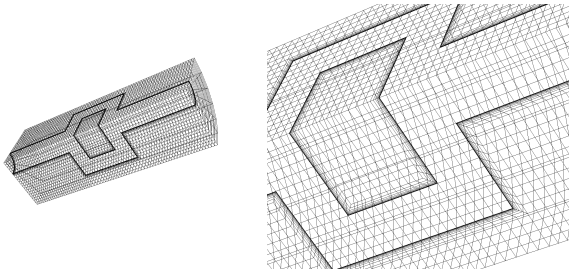


Figure 7: Left: Poisson problem on a crooked pipe mesh. Right: zoom-in of the center part of the mesh.

to generate problems of different sizes. Moreover, the maximum number of inner iterations in step 9 of Algorithm 2 is varied between three and five. We compare `parGeMSLR` against BoomerAMG with Hybrid Modified Independent Set (HMIS) coarsening, where we consider both Gauss-Seidel and l_1 Jacobi smoother [70], and report the corresponding results in Table 1. `parGeMSLR` is able to outperform Schur ILU, especially for larger problems. Moreover, the iteration time of `parGeMSLR` is similar to that of BoomerAMG with Gauss-Seidel smoother, but much lower than that of BoomerAMG with l_1 Jacobi smoother.

Table 1: Solving (10) on a crooked pipe mesh.

prec	size	n_p	k	fill	p-t	i-t	its
Boomer AMG GS	126,805	16	-	1.71	0.17	0.69	106
	966,609	32	-	1.79	0.79	5.7	198
	7,544,257	64	-	1.81	3.36	45.12	250
Boomer AMG Jacobi	126,805	16	-	1.71	0.18	1.29	226
	966,609	32	-	1.79	0.8	10.95	431
	7,544,257	64	-	1.81	3.39	72.1	568
Schur ILU	126,805	16	-	1.53	0.22	0.51	65
	966,609	32	-	1.86	1.2	12.46	383
	7,544,257	64	-	1.94	5.51	-	F
par GeMSLR	126,805	16	10	1.05	0.54	0.46	25
	966,609	32	10	1.18	3.59	4.70	53
	7,544,257	64	10	1.32	11.76	48.35	128

5.2.2. *Linear elasticity equation*

In the section we consider the solution of the following linear elasticity equation:

$$\mu\Delta u + (\lambda + \mu)\nabla(\nabla \cdot u) \quad = \quad f \ \text{ in } \Omega, \tag{11}$$

where Ω is a 3D cantilever beam as shown in Figure 8. The left

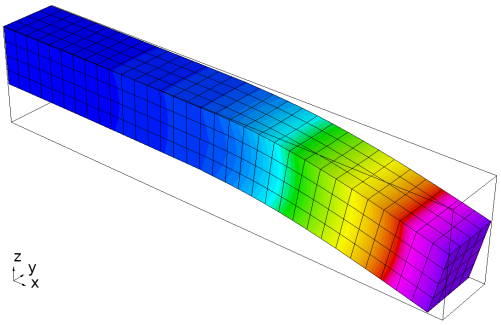


Figure 8: Linear elasticity problem on a 3D beam.

end of the beam is fixed, while a constant force (represented by f) pulls down the beam from the right end. Herein, u is the displacement, while λ and μ are the material's Lamė constants. The initial approximation is again set equal to zero in order to satisfy the boundary condition.

Tables 2 and 3 show a comparison between `parGeMSLR` and SchurILU for different uniform mesh refinements obtained using first-order Finite Element. For each mesh, the problem becomes more ill-conditioned as the ratio $\frac{\lambda}{\mu}$ grows larger. For this reason, we fix $\mu = 1$ and vary $\lambda = 10$ and $\lambda = 80$. Note that standard AMG converge slowly for this problem since it is almost singular. Concisely, `parGeMSLR` leads to considerable wall-clock time savings compared to SchurILU, even when the latter is allowed a higher level of fill-in.

5.2.3. *Helmholtz equation*

In this section we consider the complex version of `parGeMSLR` and apply it to solve the Helmholtz problem

$$-(\Delta + \omega^2)u = f \ \text{ in } \Omega = [0,1]^3, \tag{12}$$

Table 2: Comparison between two-level ILU and the GeMSLR for 3D Linear elasticity problem. $\mu = 1$ and $\lambda = 10$, Poisson ratio is $\frac{5}{11} \approx 0.455$.

prec	size	n_p	k	fill	p-t	i-t	its
Schur-ILU	2,475	4	-	2.62	0.03	0.06	49
	15,795	8	-	3.78	0.32	0.60	238
	111,843	16	-	7.81	4.80	19.05	751
	839,619	64	-	11.82	19.67	-	F
par GeMSLR	2,475	4	20	1.94	0.12	0.01	18
	15,795	8	40	3.58	0.92	0.04	23
	111,843	16	40	7.86	10.06	0.64	41
	839,619	64	80	10.05	63.25	3.13	65

Table 3: Comparison between two-level ILU and the GeMSLR for 3D Linear elasticity problem. $\mu = 1$ and $\lambda = 80$, Poisson ratio is $\frac{40}{81} \approx 0.494$.

prec	size	n_p	k	fill	p-t	i-t	its
Schur-ILU	2,475	4	-	2.21	0.03	0.26	336
	15,795	8	-	4.03	0.35	1.48	549
	111,843	16	-	8.94	6.45	-	F
	839,619	64	-	14.75	32.17	-	F
par GeMSLR	2,475	4	20	1.91	0.15	0.01	41
	15,795	8	40	3.58	1.09	0.15	75
	111,843	16	80	6.48	16.16	1.49	93
	839,619	64	120	10.31	133.2	6.15	128

where we use the Perfectly Matched Layer (PML) boundary condition [71] and set the number of points per wavelength equal to eight. We used random initial guesses.

Our first set of experiments focuses on the performance of `parGeMSLR` where the number of low-rank terms is varied as $k = \{10, 20, \ldots, 100\}$, and the number of levels is set equal to $l_{ev} = 3$. The size of the Helmholtz problem is set equal to $n = 50^3$. The maximum fill-in attributed to the low-rank correction term was roughly equal to three. Figure 9 plots the parallel wall-clock time as a function of the number of low-rank terms k while the number of MPI processes is fixed equal to sixteen. Overall, larger values of k lead to lower total and iteration times up to the point where the time increase associated with constructing the `parGeMSLR` preconditioner outweighs the gains from improving the convergence rate during the iterative solution by FGMRES. Next, we consider the same problem but

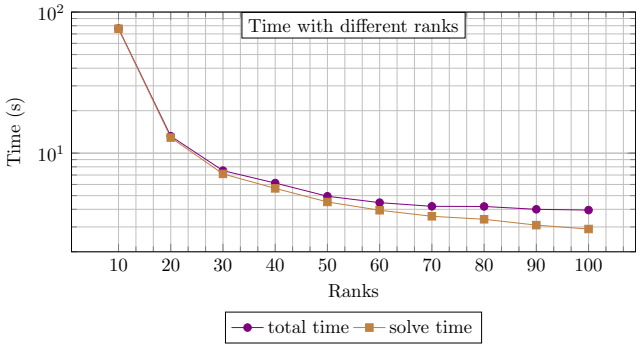


Figure 9: Total and iteration wall-clock times of the 3-level parallel GeMSLR to solve the Helmholtz equation of size $n = 50^3$ using 16 MPI processes.

Table 4: parGeMSLR with/without complex shifts for. The problem size is equal to $n = (4\omega/\pi)^3$.

	with shift							without shift		
ω	n_p	k	fill	r-t	p-t	i-t	its	fill	time	its
5π	1	0	3.40	0.04	0.02	0.05	9	3.80	0.12	9
7.5π	1	0	3.81	0.17	0.10	0.40	20	4.76	6.47	241
10π	2	5	3.52	0.43	0.41	1.03	36	4.11	15.48	449
12.5π	4	5	3.79	0.70	0.58	1.50	42	4.79	-	F
15π	8	10	4.16	1.25	1.20	2.33	55	4.63	-	F
20π	16	10	4.40	1.51	1.29	3.51	57	4.77	-	F
40π	64	20	5.49	4.87	7.84	14.43	92	5.73	-	F

this time we add a complex shift equal to $0.05i * \sum_i |A_{ii}|/n_A$ during the the ILU factorization of the on-diagonal blocks. The same idea was already considered in [72, 24, 14] but this time we apply it in the context of distributed-memory computing and make it available in parGeMSLR. Similarly to the previous references, adding a shift helps creating a more stable ILU for indefinite problems, i.e., see Table 4.

5.3. GPU acceleration of the solution phase

The parGeMSLR library can also take advantage of specialized hardware such as GPUs to speed-up numerical kernels. The current release of parGeMSLR does not support GPU computing during the setup phase of the GeMSLR preconditioner, but allows the use of GPUs during the application of the GeMSLR preconditioner, i.e., triangular substitutions and dense, rectangular matrix-vector multiplications. Nonetheless, accelerating the solution phase might still lead to significant reductions in the overall wall-clock time, e.g., when we need to solve for multiple right-hand sides.

To demonstrate these benefits, we consider a $n = 128^3$ discretization of the model problem (10) and focus on the speedup achieved during the solution phase if GPUs are enabled. We set the number of levels equal to $l_{ev} = 2$ and $l_{ev} = 3$, and vary the low-rank correction terms as $k \in \{0, 100, 200, 300, 400, 500\}$. At each level, we apply a 4-way partition and assign each partition to a separate MPI process binded to a V100 NVIDIA GPU. Figure 10 plots the speedups achieved by the hybrid CPU+GPU version of parGeMSLR during its solve phase. As expected, the peak speedup is obtained for the case $k = 500$, since the cost to apply the low-rank correction term increases linearly with the value of k.

6. Concluding remarks and future work

In this paper we presented parGeMSLR, a C++ parallel software library for the iterative solution of general sparse systems distributed among several processor groups communicating via MPI. environments [24]. parGeMSLR is based on the GeMSLR preconditioner and can be applied to both real and complex systems of linear algebraic equations. The performance of parGeMSLR on distributed-memory computing environments was demonstrated on both model and real-world problems, verifying the efficiency of the library as a general-purpose solver.

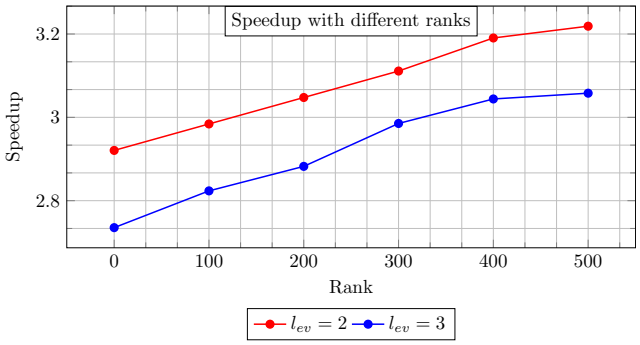


Figure 10: Speedup of the solution phase of parGeMSLR if GPU acceleration is enabled when $l_{ev} = \{2, 3\}$, and $k \in \{0, 100, 200, 300, 400, 500\}$. The problem size is equal to $n = 128^3$.

As future work we plan to replace standard Arnoldi by either its block variant or randomized subspace iteration. This should improve performance by reducing latency during the preconditioner setup phase. Moreover, the cost of the setup phase can be amortized over the solution of linear systems with multiple right-hand sides, e.g., see [73, 74, 75, 76], and we plan to apply parGeMSLR to this type of problems. In this context, we also plan to apply parGeMSLR to the solution of sparse linear systems appearing in eigenvalue solvers based on rational filtering [77, 78], and domain decomposition [79, 80].

References

[1] Y. Saad, Iterative Methods for Sparse Linear Systems, Other Titles in Applied Mathematics, Society for Industrial and Applied Mathematics, 2003. doi:10.1137/1.9780898718003.

[2] H. A. Van der Vorst, Iterative Krylov methods for large linear systems, no. 13, Cambridge University Press, 2003.

[3] Y. Saad, M. H. Schultz, GMRES: A Generalized Minimal Residual Algorithm for Solving Nonsymmetric Linear Systems, SIAM Journal on Scientific and Statistical Computing 7 (3) (1986) 856–869, publisher: Society for Industrial and Applied Mathematics. doi:10.1137/0907058.

[4] J. W. Ruge, K. St{\"u}ben, Algebraic Multigrid, in: Multigrid Methods, Frontiers in Applied Mathematics, Society for Industrial and Applied Mathematics, 1987, pp. 73–130. doi:10.1137/1.9781611971057.ch4.

[5] V. E. Henson, U. M. Yang, BoomerAMG: A parallel algebraic multigrid solver and preconditioner, Applied Numerical Mathematics 41 (1) (2002) 155–177. doi:10.1016/S0168-9274(01)00115-5.

[6] A. J. Cleary, R. D. Falgout, V. E. Henson, J. E. Jones, T. A. Manteuffel, S. F. McCormick, G. N. Miranda, J. W. Ruge, Robustness and scalability of algebraic multigrid, SIAM Journal on Scientific Computing 21 (5) (2000) 1886–1908.

[7] N. Bell, S. Dalton, L. N. Olson, Exposing fine-grained parallelism in algebraic multigrid methods, SIAM Journal on Scientific Computing 34 (4) (2012) C123–C152.

[8] Y. Saad, ILUT: A dual threshold incomplete LU factorization, Numerical Linear Algebra with Applications 1 (4) (1994) 387–402. doi:10.1002/nla.1680010405.

[9] E. Chow, Y. Saad, Experimental study of ilu preconditioners for indefinite matrices, Journal of computational and applied mathematics 86 (2) (1997) 387–414.

[10] O. G. Ernst, M. J. Gander, Why it is Difficult to Solve Helmholtz Problems with Classical Iterative Methods, in: I. G. Graham, T. Y. Hou, O. Lakkis, R. Scheichl (Eds.), Numerical Analysis of Multiscale Problems, Vol. 83, Springer Berlin Heidelberg, Berlin, Heidelberg, 2012, pp. 325–363. doi:10.1007/978-3-642-22061-6_10.

[11] X. Liu, Y. Xi, Y. Saad, M. V. de Hoop, Solving the three-dimensional high-frequency helmholtz equation using contour integration and polynomial preconditioning, SIAM Journal on Matrix Analysis and Applications 41 (1) (2020) 58–82.

[12] M. Magolu monga Made, R. Beauwens, G. Warzée, Preconditioning of discrete Helmholtz operators perturbed by a diagonal complex matrix, Communications in Numerical Methods in Engineering 16 (11) (2000) 801–817. doi:https://doi.org/10.1002/1099-0887(200011)16:11<801::AID-CNM377>3.0.CO;2-M.

[13] Y. A. Erlangga, C. Vuik, C. W. Oosterlee, Comparison of multigrid and incomplete LU shifted-Laplace preconditioners for the inhomogeneous Helmholtz equation, Applied Numerical Mathematics 56 (5) (2006) 648–666. doi:10.1016/j.apnum.2005.04.039.

[14] D. Osei-Kuffuor, Y. Saad, Preconditioning Helmholtz linear systems, Applied Numerical Mathematics 60 (4) (2010) 420–431. doi:10.1016/j.apnum.2009.09.003.

[15] H. Anzt, E. Chow, J. Dongarra, Parilut—a new parallel threshold ilu factorization, SIAM Journal on Scientific Computing 40 (4) (2018) C503–C519.

[16] H. Anzt, T. Ribizel, G. Flegar, E. Chow, J. Dongarra, Parilut-a parallel threshold ilu for gpus, in: 2019 IEEE International Parallel and Distributed Processing Symposium (IPDPS), IEEE, 2019, pp. 231–241.

[17] E. Chow, A. Patel, Fine-Grained Parallel Incomplete LU Factorization, SIAM Journal on Scientific Computing 37 (2) (2015) C169–C193. doi:10.1137/140968896.

[18] X.-C. Cai, M. Sarkis, A Restricted Additive Schwarz Preconditioner for General Sparse Linear Systems, SIAM Journal on Scientific Computing 21 (2) (1999) 792–797. doi:10.1137/S106482759732678X.

[19] D. Hysom, A. Pothen, Efficient parallel computation of ILU(k) preconditioners, in: Proceedings of the 1999 ACM/IEEE conference on Supercomputing, SC '99, Association for Computing Machinery, New York, NY, USA, 1999, pp. 29–es. doi:10.1145/331532.331561.

[20] G. Karypis, V. Kumar, Parallel Threshold-based ILU Factorization, in: Supercomputing, ACM/IEEE 1997 Conference, 1997, pp. 28–28. doi:10.1145/509593.509621.

[21] Y. Saad, J. Zhang, BILUTM: A Domain-Based Multilevel Block ILUT Preconditioner for General Sparse Matrices, SIAM Journal on Matrix Analysis and Applications 21 (1) (1999) 279–299, publisher: Society for Industrial and Applied Mathematics. doi:10.1137/S0895479898341268.

[22] Z. Li, Y. Saad, M. Sosonkina, pARMS: a parallel version of the algebraic recursive multilevel solver, Numerical Linear Algebra with Applications 10 (5-6) (2003) 485–509. doi:10.1002/nla.325.

[23] I. C. L. NIEVINSKI, M. SOUZA, P. GOLDFELD, D. A. AUGUSTO, J. R. P. RODRIGUES, L. M. CARVALHO, Parallel Implementation of a Two-level Algebraic ILU(k)-based Domain Decomposition Preconditioner, TEMA (SÃ£o Carlos) 19 (2018) 59–77, publisher: scielo. doi:10.5540/tema.2018.019.01.0059.

[24] G. Dillon, V. Kalantzis, Y. Xi, Y. Saad, A Hierarchical Low Rank Schur Complement Preconditioner for Indefinite Linear Systems, SIAM Journal on Scientific Computing 40 (4) (2018) A2234–A2252. doi:10.1137/17M1143320.

[25] J. Mandel, C. R. Dohrmann, Convergence of a balancing domain decomposition by constraints and energy minimization, Numerical linear algebra with applications 10 (7) (2003) 639–659.

[26] C. Farhat, M. Lesoinne, P. LeTallec, K. Pierson, D. Rixen, Feti-dp: a dual–primal unified feti method—part i: A faster alternative to the two-level feti method, International journal for numerical methods in engineering 50 (7) (2001) 1523–1544.

[27] A. Heinlein, A. Klawonn, M. Lanser, J. Weber, Combining machine learning and adaptive coarse spaces—a hybrid approach for robust feti-dp methods in three dimensions, SIAM Journal on Scientific Computing 43 (5) (2021) S816–S838.

[28] N. Spillane, V. Dolean, P. Hauret, F. Nataf, C. Pechstein, R. Scheichl, Abstract robust coarse spaces for systems of pdes via generalized eigenproblems in the overlaps, Numerische Mathematik 126 (4) (2014) 741–770.

[29] P. R. Amestoy, I. S. Duff, J.-Y. L'Excellent, J. Koster, Mumps: a general purpose distributed memory sparse solver, in: International Workshop on Applied Parallel Computing, Springer, 2000, pp. 121–130.

[30] P. Hénon, P. Ramet, J. Roman, Pastix: a high-performance parallel direct solver for sparse symmetric positive definite systems, Parallel Computing 28 (2) (2002) 301–321.

[31] R. Li, Y. Saad, Low-Rank Correction Methods for Algebraic Domain Decomposition Preconditioners, SIAM Journal on Matrix Analysis and Applications 38 (3) (2017) 807–828. doi:10.1137/16M110486X.

[32] E. G. Boman, L. Cambier, C. Chen, E. Darve, S. Rajamanickam, R. S. Tuminaro, A preconditioner based on sparsified nested dissection and low-rank approximation, in: XXI Householder Symposium on Numerical Linear Algebra, 2020, p. 128.

[33] M. Benzi, M. Tuma, A Sparse Approximate Inverse Preconditioner for Nonsymmetric Linear Systems, SIAM Journal on Scientific Computing 19 (3) (1998) 968–994. doi:10.1137/S1064827595294691.

[34] E. Chow, Y. Saad, Approximate Inverse Preconditioners via Sparse-Sparse Iterations, SIAM Journal on Scientific Computing 19 (3) (1998) 995–1023. doi:10.1137/S1064827594270415.

[35] C. Janna, M. Ferronato, G. Gambolati, A Block FSAI-ILU Parallel Preconditioner for Symmetric Positive Definite Linear Systems, SIAM Journal on Scientific Computing 32 (5) (2010) 2468–2484, publisher: Society for Industrial and Applied Mathematics. doi:10.1137/090779760.

[36] H. Anzt, T. K. Huckle, J. Bräckle, J. Dongarra, Incomplete sparse approximate inverses for parallel preconditioning, Parallel Computing 71 (2018) 1–22.

[37] M. J. Grote, T. Huckle, Parallel preconditioning with sparse approximate inverses, SIAM Journal on Scientific Computing 18 (3) (1997) 838–853.

[38] X. Ye, Y. Xi, Y. Saad, Preconditioning via gmres in polynomial space (2019).

[39] D. Cai, E. Chow, L. Erlandson, Y. Saad, Y. Xi, SMASH: Structured matrix approximation by separation and hierarchy, Numerical Linear Algebra with Applications 25 (6) (2018) e2204. doi:https://doi.org/10.1002/nla.2204.

[40] W. Hackbusch, A Sparse Matrix Arithmetic Based on $\Cal H$-Matrices. Part I: Introduction to ${\Cal H}$-Matrices, Computing 62 (2) (1999) 89–108. doi:10.1007/s006070050015.

[41] W. Hackbusch, B. N. Khoromskij, A Sparse $\Cal H$-Matrix Arithmetic. Part II: Application to Multi-Dimensional Problems, Computing 64 (1) (2000) 21–47. doi:10.1007/PL00021408.

[42] Y. Xi, J. Xia, S. Cauley, V. Balakrishnan, Superfast and Stable Structured Solvers for Toeplitz Least Squares via Randomized Sampling, SIAM Journal on Matrix Analysis and Applications 35 (1) (2014) 44–72, publisher: Society for Industrial and Applied Mathematics. doi:10.1137/120895755.

[43] C. Chen, H. Pouransari, S. Rajamanickam, E. G. Boman, E. Darve, A distributed-memory hierarchical solver for general sparse linear systems, Parallel Computing 74 (2018) 49–64.

[44] R. Li, Y. Xi, Y. Saad, Schur complement-based domain decomposition preconditioners with low-rank corrections, Numerical Linear Algebra with Applications 23 (4) (2016) 706–729. doi:10.1002/nla.2051.

[45] R. D. Falgout, U. M. Yang, hypre: A Library of High Performance Preconditioners, in: P. M. A. Sloot, A. G. Hoekstra, C. J. K. Tan, J. J. Dongarra (Eds.), Computational Science ICCS 2002, Lecture Notes in Computer Science, Springer, Berlin, Heidelberg, 2002, pp. 632–641. doi:10.1007/3-540-47789-6_66.

[46] P. Labs, Paralution v1.1.0, http://www.paralution.com/ (2016).

[47] K. Rupp, P. Tillet, F. Rudolf, J. Weinbub, A. Morhammer, T. Grasser, A. Jungel, S. Selberherr, Viennacl—linear algebra library for multi-and many-core architectures, SIAM Journal on Scientific Computing 38 (5) (2016) S412–S439.

[48] S. Gawlok, P. Gerstner, S. Haupt, V. Heuveline, J. Kratzke, P. Lösel, K. Mang, M. Schmidtobreick, N. Schoch, N. Schween, J. Schwegler, C. Song, M. Wlotzka, Hiflow3 – technical report on release 2.0, Preprint Series of the Engineering Mathematics and Computing Lab (EMCL) 0 (06) (2017). doi:10.11588/emclpp.2017.06.42879.

[49] S. Balay, K. Buschelman, W. D. Gropp, D. Kaushik, M. G. Knepley, L. C. McInnes, B. F. Smith, H. Zhang, Petsc, See http://www. mcs. anl. gov/petsc (2001).

[50] T. Trilinos Project Team, The Trilinos Project Website.

[51] P. Ghysels, S. L. Xiaoye, C. Gorman, F.-H. Rouet, A robust parallel preconditioner for indefinite systems using hierarchical matrices and randomized sampling, in: 2017 IEEE International Parallel and Distributed Processing Symposium (IPDPS), IEEE, 2017, pp. 897–906.

[52] P. Ghysels, X. S. Li, F.-H. Rouet, S. Williams, A. Napov, An efficient multicore implementation of a novel hss-structured multifrontal solver us-

ing randomized sampling, SIAM Journal on Scientific Computing 38 (5) (2016) S358–S384.
[53] F.-H. Rouet, X. S. Li, P. Ghysels, A. Napov, A distributed-memory package for dense hierarchically semi-separable matrix computations using randomization, ACM Transactions on Mathematical Software (TOMS) 42 (4) (2016) 1–35.
[54] X. S. Li, J. W. Demmel, SuperLU_DIST: A scalable distributed-memory sparse direct solver for unsymmetric linear systems, ACM Trans. Mathematical Software 29 (2) (2003) 110–140.
[55] L. Grigori, F. Nataf, S. Yousef, Robust algebraic Schur complement preconditioners based on low rank corrections, Research Report RR-8557, INRIA (Jul. 2014).
[56] Y. Xi, R. Li, Y. Saad, An Algebraic Multilevel Preconditioner with Low-Rank Corrections for Sparse Symmetric Matrices, SIAM Journal on Matrix Analysis and Applications 37 (1) (2016) 235–259. doi:10.1137/15M1021830.
[57] S. Rajamanickam, E. G. Boman, M. A. Heroux, Shylu: A hybrid-hybrid solver for multicore platforms, in: 2012 IEEE 26th International Parallel and Distributed Processing Symposium, IEEE, 2012, pp. 631–643.
[58] H. A. Daas, T. Rees, J. Scott, Two-level nystr\" om–schur preconditioner for sparse symmetric positive definite matrices, arXiv preprint arXiv:2101.12164 (2021).
[59] G. Karypis, V. Kumar, A Fast and High Quality Multilevel Scheme for Partitioning Irregular Graphs, SIAM Journal on Scientific Computing 20 (1) (1998) 359–392, publisher: Society for Industrial and Applied Mathematics. doi:10.1137/S1064827595287997.
[60] U. V. Catalyurek, C. Aykanat, Hypergraph-partitioning-based decomposition for parallel sparse-matrix vector multiplication, IEEE Transactions on Parallel and Distributed Systems 10 (7) (1999) 673–693. doi:10.1109/71.780863.
[61] B. Hendrickson, R. Leland, The Chaco User's Guide Version 2, Sandia National Laboratories, Albuquerque NM (1994).
[62] F. Pellegrini, Scotch and libScotch 5.1 User's Guide, INRIA Bordeaux Sud-Ouest, IPB & LaBRI, UMR CNRS 5800 (2010).
[63] P. Hénon, Y. Saad, A parallel multistage ilu factorization based on a hierarchical graph decomposition, SIAM Journal on Scientific Computing 28 (6) (2006) 2266–2293.
[64] P. R. Amestoy, T. A. Davis, I. S. Duff, An Approximate Minimum Degree Ordering Algorithm, SIAM Journal on Matrix Analysis and Applications 17 (4) (1996) 886–905, publisher: Society for Industrial and Applied Mathematics. doi:10.1137/S0895479894278952.
[65] A. George, J. W. Liu, Computer Solution of Large Sparse Positive Definite, Prentice Hall Professional Technical Reference, 1981.
[66] A. Bienz, W. D. Gropp, L. N. Olson, Node aware sparse matrix–vector multiplication, Journal of Parallel and Distributed Computing 130 (2019) 166–178.
[67] R. Anderson, J. Andrej, A. Barker, J. Bramwell, J.-S. Camier, J. C. V. Dobrev, Y. Dudouit, A. Fisher, T. Kolev, W. Pazner, M. Stowell, V. Tomov, I. Akkerman, J. Dahm, D. Medina, S. Zampini, MFEM: A modular finite element library, Computers & Mathematics with Applications (2020). doi:10.1016/j.camwa.2020.06.009.
[68] MFEM: Modular finite element methods [Software], mfem.org. doi:10.11578/dc.20171025.1248.
[69] GLVis: Opengl finite element visualization tool, glvis.org. doi:10.11578/dc.20171025.1249.
[70] A. H. Baker, R. D. Falgout, T. V. Kolev, U. M. Yang, Multigrid Smoothers for Ultraparallel Computing, SIAM Journal on Scientific Computing 33 (5) (2011) 2864–2887, publisher: Society for Industrial and Applied Mathematics. doi:10.1137/100798806.
[71] X. Liu, Y. Xi, Y. Saad, M. V. de Hoop, Solving the 3d high-frequency helmholtz equation using contour integration and polynomial preconditioning, arXiv preprint arXiv:1811.12378 (2018).
[72] Y. A. Erlangga, C. Vuik, C. W. Oosterlee, On a class of preconditioners for solving the helmholtz equation, Applied Numerical Mathematics 50 (3-4) (2004) 409–425.
[73] V. Simoncini, E. Gallopoulos, An iterative method for nonsymmetric systems with multiple right-hand sides, SIAM Journal on Scientific Computing 16 (4) (1995) 917–933.
[74] A. Hussam, L. GRIGORI, P. Hénon, P. RICOUX, Enlarged gmres for solving linear systems with one or multiple right-hand sides.
[75] V. Kalantzis, C. Bekas, A. Curioni, E. Gallopoulos, Accelerating data uncertainty quantification by solving linear systems with multiple right-hand sides, Numerical Algorithms 62 (4) (2013) 637–653.
[76] V. Kalantzis, A. C. I. Malossi, C. Bekas, A. Curioni, E. Gallopoulos, Y. Saad, A scalable iterative dense linear system solver for multiple right-hand sides in data analytics, Parallel Computing 74 (2018) 136–153.
[77] V. Kalantzis, Y. Xi, L. Horesh, Fast randomized non-hermitian eigensolvers based on rational filtering and matrix partitioning, SIAM Journal on Scientific Computing 43 (5) (2021) S791–S815. arXiv:https://doi.org/10.1137/20M1349217, doi:10.1137/20M1349217.
[78] Y. Xi, Y. Saad, Computing Partial Spectra with Least-Squares Rational Filters, SIAM Journal on Scientific Computing 38 (5) (2016) A3020–A3045. doi:10.1137/16M1061965.
[79] V. Kalantzis, Y. Xi, Y. Saad, Beyond automated multilevel substructuring: Domain decomposition with rational filtering, SIAM Journal on Scientific Computing 40 (4) (2018) C477–C502. arXiv:https://doi.org/10.1137/17M1154527, doi:10.1137/17M1154527.
[80] V. Kalantzis, A domain decomposition rayleigh–ritz algorithm for symmetric generalized eigenvalue problems, SIAM Journal on Scientific Computing 42 (6) (2020) C410–C435.